Title

Efficient meltwater drainage through supraglacial streams and rivers on the southwest Greenland ice sheet.

Journal

Proceedings of the National Academy of Sciences of the United States of America, 112(4)

ISSN

0027-8424

Authors

Smith, Laurence C
Chu, Vena W
Yang, Kang
et al.

Publication Date

2015

DOI

10.1073/pnas.1413024112

Peer reviewed

Efficient meltwater drainage through supraglacial streams and rivers on the southwest Greenland ice sheet

Laurence C. Smith[a,1], Vena W. Chu[a], Kang Yang[a], Colin J. Gleason[a], Lincoln H. Pitcher[a], Asa K. Rennermalm[b], Carl J. Legleiter[c], Alberto E. Behar[d,2], Brandon T. Overstreet[c], Samiah E. Moustafa[b], Marco Tedesco[e], Richard R. Forster[f], Adam L. LeWinter[g], David C. Finnegan[g], Yongwei Sheng[a], and James Balog[h]

[a]Department of Geography, University of California, Los Angeles, CA 90095; [b]Department of Geography, Rutgers University, Piscataway, NJ 08854; [c]Department of Geography, University of Wyoming, Laramie, WY 82071; [d]NASA Jet Propulsion Laboratory, Pasadena, CA 91109; [e]Department of Earth and Atmospheric Science, The City College of New York, NY, 10031; [f]Department of Geography, University of Utah, Salt Lake City, UT 84112; [g]U.S. Army Cold Regions Research & Engineering Laboratory, Hanover, NH 03755; and [h]Earth Vision Trust, Boulder, CO 80304

Edited by John H. England, University of Alberta, Edmonton, Canada, and accepted by the Editorial Board November 13, 2014 (received for review July 10, 2014)

Thermally incised meltwater channels that flow each summer across melt-prone surfaces of the Greenland ice sheet have received little direct study. We use high-resolution WorldView-1/2 satellite mapping and in situ measurements to characterize supraglacial water storage, drainage pattern, and discharge across 6,812 km^2 of southwest Greenland in July 2012, after a record melt event. Efficient surface drainage was routed through 523 high-order stream/river channel networks, all of which terminated in moulins before reaching the ice edge. Low surface water storage (3.6 ± 0.9 cm), negligible impoundment by supraglacial lakes or topographic depressions, and high discharge to moulins (2.54–2.81 cm·d^{-1}) indicate that the surface drainage system conveyed its own storage volume every <2 d to the bed. Moulin discharges mapped inside ∼52% of the source ice watershed for Isortoq, a major proglacial river, totaled ∼41–98% of observed proglacial discharge, highlighting the importance of supraglacial river drainage to true outflow from the ice edge. However, Isortoq discharges tended lower than runoff simulations from the Modèle Atmosphérique Régional (MAR) regional climate model (0.056–0.112 km^3·d^{-1} vs. ∼0.103 km^3·d^{-1}), and when integrated over the melt season, totaled just 37–75% of MAR, suggesting nontrivial subglacial water storage even in this melt-prone region of the ice sheet. We conclude that (*i*) the interior surface of the ice sheet can be efficiently drained under optimal conditions, (*ii*) that digital elevation models alone cannot fully describe supraglacial drainage and its connection to subglacial systems, and (*iii*) that predicting outflow from climate models alone, without recognition of subglacial processes, may overestimate true meltwater export from the ice sheet to the ocean.

Greenland ice sheet | supraglacial hydrology | meltwater runoff | mass balance | remote sensing

Meltwater runoff from the Greenland ice sheet (GrIS) accounts for half or more of its total mass loss to the global ocean (1, 2) but remains one of the least-studied hydrologic processes on Earth. Each summer, a complex system of supraglacial meltwater ponds, lakes, streams, rivers, and moulins develops across large areas of the southwestern GrIS surface, especially below ∼1,300 m elevation (3–7), with supraglacial erosion driven by thermal and radiative processes (5). Digital elevation models (DEMs) suggest a poorly drained surface resulting from abundant topographic depressions, which computational flow routing models must artificially "fill" to allow hydrological flow paths extending from the ice sheet interior to its edge (8–11). The realism of such modeled flow paths remains largely untested by real-world observations.

To date, most observational studies of GrIS supraglacial hydrology have focused on large lakes (∼1 km^2) because of their good visibility in commonly available optical satellite images (6, 12–15). Lakes have also attracted considerable scientific interest because some of them can abruptly drain, rapidly transferring water from the supraglacial to the subglacial system, triggering transient ice uplift and velocity changes (16–20). Greenland's large supraglacial channels (Fig. 1), however, have received much less study, despite their acknowledged role as a transport mechanism for meltwater and their linkage to englacial/subglacial systems via moulins, crevasses, and shear fractures (21, 22). Reasons for this include difficulties in remote sensing of narrow supraglacial channels (22) and lack of in situ hydraulic data because of challenging field conditions in the ablation zone, where a rapidly lowering ice surface, abundant flowing water, and dangerously fast currents limit mobility and instrument installations. For these reasons, large supraglacial streams are not well characterized, and their overall drainage pattern, storage capacity, discharge, and comparative importance as a GrIS supraglacial runoff mechanism are unknown. In turn, this knowledge gap impedes process-level understanding of ice sheet mass losses from meltwater runoff, which have accelerated since 2000 (2, 23) and are expected to rise further in the future (24–26).

Significance

Meltwater runoff from the Greenland ice sheet is a key contributor to global sea level rise and is expected to increase in the future, but it has received little observational study. We used satellite and in situ technologies to assess surface drainage conditions on the southwestern ablation surface after an extreme 2012 melting event. We conclude that the ice sheet surface is efficiently drained under optimal conditions, that digital elevation models alone cannot fully describe supraglacial drainage and its connection to subglacial systems, and that predicting outflow from climate models alone, without recognition of subglacial processes, may overestimate true meltwater release from the ice sheet.

Author contributions: L.C.S. conceived the project; L.C.S., V.W.C., K.Y., C.J.G., L.H.P., A.K.R., C.J.L., and Y.S. designed research; A.E.B., A.L.L., D.C.F., and J.B. designed instrumentation; L.C.S., V.W.C., K.Y., C.J.G., L.H.P., A.K.R., C.J.L., A.E.B., B.T.O., S.E.M., M.T., R.R.F., A.L.L., and D.C.F. performed field work; V.W.C., K.Y., C.J.G., and L.H.P. conducted analyses; L.C.S. wrote the paper; and V.W.C., K.Y., C.J.G., and L.H.P. helped write the paper.

The authors declare no conflict of interest.

This article is a PNAS Direct Submission. J.H.E. is a guest editor invited by the Editorial Board.

Freely available online through the PNAS open access option.

[1]To whom correspondence should be addressed. Email: lsmith@geog.ucla.edu.

[2]Deceased January 9, 2015.

This article contains supporting information online at www.pnas.org/lookup/suppl/doi:10.1073/pnas.1413024112/-/DCSupplemental.

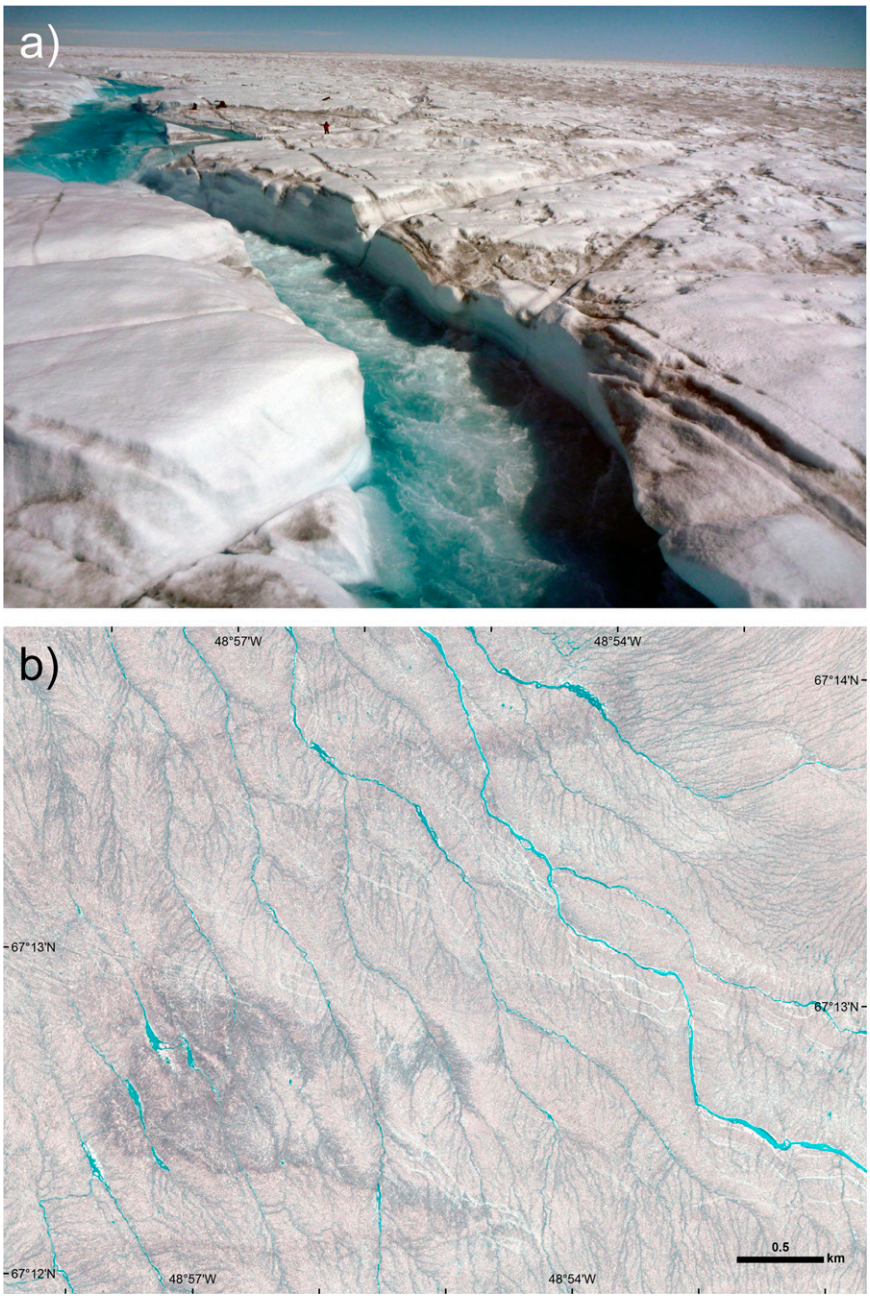

Fig. 1. Supraglacial river networks represent an important high-capacity mechanism for conveying large volumes of meltwater across the GrIS surface, as illustrated by (*A*) 23 July 2012 field photo (see authors in the image for scale), and (*B*) same-day WV2 satellite image. Both images were acquired ~55 km inland of the ice edge near Kangerlussuaq, southwest Greenland.

A possible foreshadow of such a future was a record 11–13 July 2012 melt event that briefly thawed 97% of the GrIS surface (27, 28). Here, we use high-resolution WorldView-2 (WV2) and WorldView-1 (WV1) satellite images, together with contemporaneous in situ field measurements, to study the surface drainage pattern, storage capacity, discharge, and ultimate fate of meltwater generated across a 6,812 km^2 melt-vulnerable area of the southwest GrIS immediately after this rare event. As such, the goal of the study is to characterize supraglacial drainage conditions for an important runoff-producing region of the ice sheet during peak melting conditions and should be viewed as an end-member situation, rather than as universally descriptive of the broader ice sheet. This area also produces some of Greenland's largest proglacial rivers (e.g., Isortoq, Watson, Kûk, Qordlotoq) and offers logistics support from the nearby community of Kangerlussuaq.

During a 6-d mapping period (18–23 July 2012), surface water bodies in this area were mapped at high resolution (2 m) from 32 multispectral WV2 images, all acquired during the peak of the daily melt cycle between 13:53 and 14:09 local time. At the same time, field teams collected supporting in situ hydraulic measurements from nine positions on the ice sheet, including thousands of colocated water depths and spectral reflectances from a customized unmanned surface vessel, flow velocities from drifting autonomous Global Positioning System beacons and portable Doppler radars, cross-sectional velocity fields from an Acoustic Doppler Current Profiler, and channel flow widths, depths, slopes, roughness coefficients, and hydraulic geometry from traditional

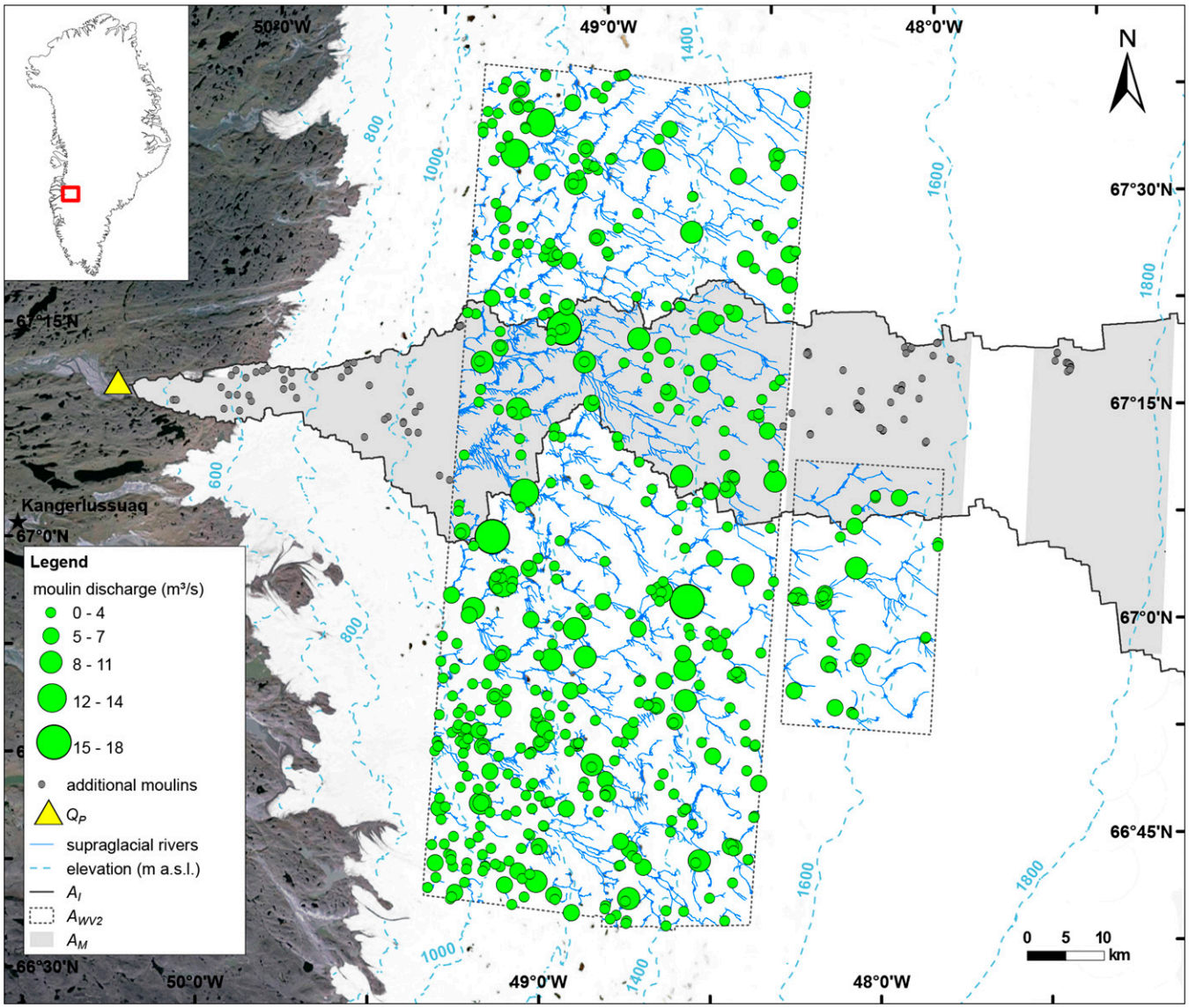

Fig. 2. Five hundred twenty-three supraglacial river networks, their terminal moulin locations, and moulin discharges were mapped from 32 multispectral WV2 images, with calibration from contemporaneous field measurements collected on the ice sheet (18–23 July 2012). An additional 102 moulins were mapped from panchromatic WV1 imagery (black circles). Downstream discharges from the proglacial river Isortoq were also observed (yellow triangle). All mapped supraglacial rivers terminated in moulins (green circles, with diameters proportional to estimated meltwater flux), with negligible water impoundment in depressions and supraglacial lakes on the ice sheet surface.

terrestrial field survey methods. These measurements were needed to characterize the hydraulic properties of supraglacial melt channels and to calibrate two empirical remote-sensing algorithms for WV2 estimation of water depth and discharge, respectively. An additional 20 WV1 panchromatic images (0.5 m resolution) acquired on 20, 21, 25, 30, and 31 July and 12 August between 12:49 and 14:19 local time were used to map moulin locations at higher and lower elevations on the ice sheet (~300–1,800 m above sea level) and to elucidate physical mechanisms for their formation. Instantaneous river moulin discharges were estimated from WV2 using field-calibrated hydraulic geometry coefficients, and channel morphology metrics were derived from WV2 and WV1 using standard watershed analysis tools in ArcGIS. Downstream of the study area, ongoing proglacial river discharges were collected from Isortoq, one of Greenland's largest oceangoing terrestrial rivers that emerges from the ice edge, using field-calibrated time-lapse photography of braid plain inundation area. The ice watershed of Isortoq makes up a smaller subset of our broader study area and was delineated from available surface and basal topography DEMs, using different methods and DEM resolutions, to quantify watershed delineation uncertainty. Finally, to understand the overall importance of supraglacial rivers as an enabling mechanism for supra- and proglacial water transport, their sum total discharge delivered to moulins was compared with surface mass balance-based calculations of melt production and runoff from the Modèle Atmosphérique Régional (MAR) regional climate model (25), as well as the downstream proglacial river discharges observed in Isortoq. Three study areas were examined for this purpose: the mapped WV2 mosaic in its entirety (A_{WV2}, 5,328 km^2), the activated (i.e., thawed, runoff-producing) area of the Isortoq watershed (A_I, which averaged 4,941 km^2 during the 18–23 July 2012 WV2 mapping period), and a 2,574 km^2 (~52%) subset of A_I imaged by WV2 and WV1 for the purpose of moulin mapping A_M (Fig. 2). For descriptions of data products, image processing, field methods, analyses, and uncertainty quantification, see *SI Materials and Methods* and Figs. S1–S8.

Supraglacial Drainage Pattern, Stream/River Networks, and Moulins

The high-resolution mapping derived from the 18–23 July 2012 WV2 multispectral satellite mapping campaign revealed an exceedingly well-drained surface with 523 densely spaced, coalescent supraglacial stream networks characterized by dendritic, parallel, and/or centripetal drainage patterns (Fig. 2). In total, some 5,928 km of large streams were delineated within the WV2 mapped area A_{WV2}, using an automated extraction method (22). Strahler stream orders ranged from 1 to 5, and drainage densities (D_d) ranged from 0.9 to 4.8 km/km^2, with a weak linear trend of declining D_d with higher elevation. Bifurcation ratios (R_b) averaged 3.7 ± 1.9, approaching the lower range of terrestrial systems (3.0–5.0) and indicating a homogenous substrate. Inclusion of smaller streams manually digitized within two subcatchments (*WV1/2 Images and Data Processing*; Fig. S3) yields even higher values of stream order (1–6) and D_d (6.0–31.7 km/km^2). Such high stream orders for the main-stem channels, together with their high measured velocities (0.2–9.4 m/s), striking blue color, and multiyear stability (Fig. S4), evoke our use of the term "supraglacial river" when referring to these structures, and "supraglacial stream" for their more transient, lower-order feeder tributaries.

All 523 mapped stream/river networks terminated in actively flowing moulins (Fig. 2). The locations of these moulins were geographically dispersed and bore little relation to topographic lows, with 78% lying outside of surface depressions (>0.15 km^2), and 92% lying outside of major drained lake basins mapped in Advanced Spaceborne Thermal Emission and Reflection Radiometer satellite imagery (*WV1/2 Images and Data Processing*). The mapped river channels only nominally followed topographic relief, often breaching ice divides. Runoff flowing to lower elevations did not first fill topographic depressions, contrary to a key assumption of terrestrial watershed models [i.e., that depressions must fill with meltwater before overtopping (8, 10)]. Additional manual digitizing of 102 moulins at higher and lower elevations from panchromatic WV1 imagery identifies a weakly inverse relationship between elevation and moulin density, with 16% of river moulins observed to terminate in or near crevasse fields, 3% in drained lake basins, 45% near shear fractures, and 36% displaying no readily visible mechanism for moulin formation (Figs. S1 and S2). Viewed collectively, these observations indicate that DEMs alone cannot fully describe GrIS supraglacial drainage or its moulin connections to englacial/subglacial systems. Finally, laterally draining outlet rivers were observed to flow from all large supraglacial lakes within the A_{WV2} study area, signifying that these prominent features, which would otherwise appear to be impounding meltwater runoff in coarser resolution satellite imagery, presented little obstruction to the lateral passage of meltwater through the supraglacial hydrologic system. In sum, our findings of dense, well-integrated surface drainage pattern, little to no retention in lakes and topographic depressions, and 100% river termination in moulins signify that the surface drainage system was efficiently routing newly generated meltwater to the subsurface in the days after the 2012 melt event.

Supraglacial Meltwater Depth, Storage, and Discharge

Water depths of all supraglacial streams, rivers, ponds, and lakes mapped within the 5,328 km^2 WV2 study area A_{WV2} were derived at 2-m resolution from field-calibrated WV2 reflectance, after atmospheric correction and an optimal band ratio analysis (29). The fractional area covered by surface water totaled 72.7 km^2 (1.4% of A_{WV2}), with typical depths ranging from 0.6 to 3.4 m and a mean depth of 2.0 m. Spatial summation of these high-resolution water depth data yields a total supraglacial storage estimate of 0.19 ± 0.05 km^3 liquid water by volume (equivalent to 3.6 ± 0.9 cm average depth across A_{WV2}) for the 18–23 July 2012 mapping period.

A field-calibrated hydraulic geometry relationship relating instantaneous supraglacial river discharge (Q_S) to its wetted surface flow width was also applied to the WV2 map, enabling Q_S retrievals at thousands of locations along the delineated river networks. Immediately upstream of each river's terminal moulin, a subset of these Q_S retrievals was spatially averaged within a 1,000-m moving window (along single-thread river reaches only), to obtain 523 moulin discharge estimates ranging from 0.36 to 17.72 m^3·s^{-1} (3.56 m^3·s^{-1} uncertainty), with a mean value of 3.15 m^3·s^{-1} (*Supraglacial Channel Hydraulics and Discharge Estimation*; Fig. S6). A comparison of multitemporal Q_S retrievals from two overlapping WV2 orbit tracks shows that stable flow conditions were preserved between satellite acquisitions (Fig. S7). Summation of these derived discharges across the entire mapped study area A_{WV2} yields a total moulin flux envelope (including uncertainty) of 0.135–0.150 km^3·d^{-1} (or 2.54–2.81 cm·d^{-1}) injected into the ice sheet.

The large magnitude of this supraglacial river flux dwarfs observed supraglacial water storage. It is equivalent, for example, to refilling every mapped lake, pond, stream, and river within the 5,328 km^2 A_{WV2} study area (WV2 volume estimate 0.19 ± 0.05 km^3) in just 0.9–1.8 d. Such a discrepancy between low observed supraglacial storage capacity and large observed supraglacial river flux again signifies the efficient evacuation of meltwater through well-organized, hydraulically efficient stream/river channel networks.

Comparison of Field and Remotely Sensed Observations with Runoff Estimates from the MAR Regional Climate Model

The broader importance of this large observed supraglacial river flux becomes apparent when compared with surface mass balance-based estimates of melt production (M) and surface runoff (R) from the MAR regional climate model and a longer record of observed proglacial discharges (Q_P) collected for the Isortoq, a major oceangoing proglacial river that emerges from the ice edge downstream of the study area (with 138 observations acquired between 23 July 2011 and 1 August 2013). In addition to providing some relative context for the 18–23 July supraglacial discharge conditions, the Q_P time series also provides a longer, independent test of the standard practice of using regional climate models to infer GrIS meltwater outflow to the global ocean (and thus one component of its net contribution to sea level rise, after precipitation and refreezing are considered). A comparison of Q_P and R, for example, may yield useful insight about possible englacial/subglacial water storages within the ice sheet, a process not currently recognized in regional climate models.

During the 18–23 July 2012 study period, MAR simulations of R averaged 0.168 km^3·d^{-1} (or 3.16 cm·d^{-1} average water depth) across A_{WV2}. This signifies that supraglacial river networks were transporting 76–83% modeled ice sheet runoff R within A_{WV2} and were, thus, effective conduits for the evacuation of meltwater produced on the GrIS surface. Within the smaller 2,574 km^2 mapped subarea of the Isortoq watershed A_M, the total WV2 moulin flux envelope was 0.021–0.026 km^3·d^{-1}, rising to 0.046–0.054 km^3·d^{-1} if the aforementioned mean moulin discharge of 3.15 m^3·s^{-1} is applied to 98 additional moulins mapped in WV1 imagery (black circles, Fig. 2). Downstream, proglacial discharge Q_P averaged 0.056–0.112 km^3·d^{-1} (given the uncertainty of the photogrammetric method). Therefore, despite draining just 52% of the Isortoq river's activated ice watershed A_I, the supraglacial river moulins mapped in A_M were supplying 41–98% of its proglacial discharge, representing a significant conduit linking the interior GrIS ablation surface to subglacial, proglacial, and oceanic systems.

This efficient meltwater release was not evident from June to early July 2012, when proglacial outflow Q_p displayed minimal response to upstream M and R over its activated watershed

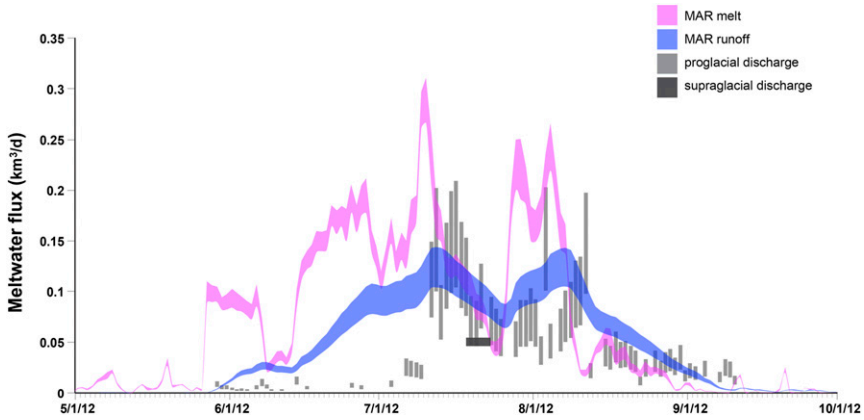

Fig. 3. Comparison of 2012 simulated meltwater production *M* (magenta) and runoff *R* (blue) from the MAR regional climate model, observed proglacial discharge (outflow) exiting the ice sheet in the Isortoq river (vertical gray bars, spanning measurement uncertainty), and total supraglacial river moulin discharge estimated for ∼52% of the Isortoq ice watershed during 18–23 July 2012 (dark gray box, spanning measurement uncertainty). Observed proglacial outflows are lower than MAR modeled runoff, especially in June. A record melt on the ice sheet occurred 11–13 July 2012.

surface, despite substantial increases in both (Fig. 3). One explanation for this may be temporary water retention in wet snow and slush, which is often observed in early-season satellite imagery (22) (Fig. S4). However, this effect is transient, with supraglacial stream/river networks in this area of southwest Greenland observed to be up and running by 15 July every year examined (e.g., 2012, 2013, and 2014; *Water Depth and Storage Estimation*; Fig. S4). The associated water deficit did not appear in Isortoq in subsequent weeks or the following spring. Integrating Q_P over the full melt season (9 May–10 September 2012) yields a total observed outflow volume that is lower than the corresponding volume of MAR modeled runoff *R* (i.e., 2.68–5.41 km^3 vs. 7.20 km^3, or 37–75%). Similarly, temporally interpolated Q_P over the maximum data collection period (23 July 2011–1 August 2013) totaled 4.42–8.93 km^3 for observations vs. 10.90 km^3 for MAR (41–82%). Even assuming maximum watershed uncertainty (*Isortoq Discharge and Watershed Delineation*; Fig. S8), the integrated Q_P over this period is 8.65–11.98 km^3 (37–103%) of MAR runoff. Alternate calculations with no interpolation of daily Q_P yields comparable results (*MAR Regional Climate Model*). This discrepancy between observed Q_p and modeled *R* suggests that either MAR overpredicts surface melting (an explanation not supported by our in situ ablation-stake measurements; *MAR Regional Climate Model*) or, more likely, that subglacial water retention processes were at play (30); for example, moulin connections to unchannelized parts of the subglacial hydrologic system (31), perhaps interrupted by dynamic switching from cavity to channel basal flow mode (18). Either explanation, especially for such a well-drained, melt-prone area of the ice sheet (13) in an unusually warm year (15), conservatively suggests that runoff simulations from atmospheric models alone, without consideration of englacial/subglacial storages, may overestimate true, oceangoing outflow in other colder, snowier parts of Greenland as well.

The extreme 2012 melt event, however, established reasonable convergence between modeled Isortoq watershed *R* and observed proglacial discharge Q_p (Fig. 3). By 11 July, proglacial discharge rose in the Isortoq River (and also in the Watson River ∼13 km to the south, where record flooding destroyed a major bridge in Kangerlussuaq), reaching a peak discharge envelope of 0.104–0.209 $km^3 \cdot d^{-1}$ on 16 July. During the 18–23 July mapping period, there was approximate congruence between Q_P (0.056–0.112 $km^3 \cdot d^{-1}$) and *R* (0.081–0.111 $km^3 \cdot d^{-1}$), attributed in part to supraglacial river fluxes from ∼52% of its watershed (0.045–0.054 $km^3 \cdot d^{-1}$). Thereafter, Q_P continued to track *R* timing for the remainder of the melt season, although at a slightly lower level (Fig. 3). This general agreement between observed Q_p and corresponding upstream modeled *R* lends qualitative support to the use of atmospheric models to estimate oceangoing discharge during highly developed drainage conditions, such as occurred here after the 2012 melt event and may become more pervasive in the future (25, 26).

On a deeper level, this research highlights the importance of hydrological processes for inclusive understanding of meltwater losses from melt-prone areas of the GrIS. Our observations show that supraglacial stream/river networks are powerful evacuators of water generated from surface melting, and in the days after the extreme 2012 melt event, neither topographic depressions on the ice surface, supraglacial lakes, nor subglacial storage presented serious obstacles to the efficient transfer of this water toward the bed and proglacial zone. Whether the extent and density of the stream/river networks mapped here were also extraordinary warrants further study, but visual inspection of eight other WV1/WV2 images from other times and years strongly suggests that the processes reported here are recurrent and annual (Fig. S4). Dynamic models of ice flow should therefore consider the injection of large water and heat fluxes through supraglacial river moulins (16, 21, 32), which, this study suggests, can only be mapped through high-resolution remote sensing. Finally, these unusual stream systems invite theoretical study from the broader river modeling/fluvial geomorphology community, in addition to glaciologists interested in process-level understanding of meltwater mass losses from the ice sheet.

With regard to GrIS mass losses, a direct comparison between modeled MAR runoff and gravity recovery and climate experiment (GRACE) gravity anomalies cannot be made for the narrow Isortoq watershed, but a similar discrepancy between regional climate model runoff simulations and GRACE gravity anomalies was evident in Greenland's southwest sector over the period 2002–2010 [i.e., −66 Gt/y surface mass balance vs. −45 ±8 Gt/yr for GRACE (table 2 in ref. 33)]. This lends further support to our contention that model-based runoff estimates may be higher than true outflow for this important runoff-producing region of the ice sheet, especially in June. Runoff assessments based on regional climate model output should thus consider additional, time-varying retention of meltwater in englacial/subglacial systems or risk overestimating true Greenland meltwater outflow to proglacial areas and the global ocean.

ACKNOWLEDGMENTS. This research is dedicated to the memory of Dr. Alberto Behar, who tragically passed away January 9, 2015. This research

was supported by the NASA Cryosphere Program (Grant NNX11AQ38G), managed by Dr. Thomas Wagner. P. Morin and C. Porter of the Polar Geospatial Center, University of Minnesota, provided WorldView-2 satellite images, tasking, and code for data processing. Updated surface and basal topography datasets were kindly provided by I. Howat (Ohio State University) and J. Bamber (University of Bristol). Careful, constructive reviews by the external readers led to substantial improvements in the finished manuscript. Field logistical support was provided by CH2M Hill Polar Field Services, the Kangerlussuaq International Science Station, and Air Greenland.

1. van den Broeke M, et al. (2009) Partitioning recent Greenland mass loss. *Science* 326(5955):984–986.
2. Enderlin EM, et al. (2014) An improved mass budget for the Greenland ice sheet. *Geophys Res Lett* 41:866–872.
3. Liang Y-L, et al. (2012) A decadal investigation of supraglacial lakes in West Greenland using a fully automatic detection and tracking algorithm. *Remote Sens Environ* 123:127–138.
4. Colgan W, et al. (2011) An increase in crevasse extent, West Greenland: Hydrologic implications. *Geophys Res Lett* 38:1–7.
5. McGrath D, Colgan W, Steffen K, Lauffenburger P, Balog J (2011) Assessing the summer water budget of a moulin basin in the Sermeq Avannarleq ablation region, Greenland ice sheet. *J Glaciol* 57:954–964.
6. Joughin I, et al. (2013) Influence of ice-sheet geometry and supraglacial lakes on seasonal ice-flow variability. *Cryosph* 7:1185–1192.
7. Lampkin DJ, VanderBerg J (November 20, 2013) Supraglacial melt channel networks in the Jakobshavn Isbræ region during the 2007 melt season. *Hydrol Process*, 10.1002/hyp.10085.
8. Arnold NS (2010) A new approach for dealing with depressions in digital elevation models when calculating flow accumulation values. *Prog Phys Geogr* 34:781–809.
9. Lewis SM, Smith LC (2009) Hydrologic drainage of the Greenland Ice Sheet. *Hydrol Processes* 23:2004–2011.
10. Banwell AF, Arnold NS, Willis IC, Tedesco M, Ahlstrøm AP (2012) Modeling supraglacial water routing and lake filling on the Greenland Ice Sheet. *J Geophys Res* 117: F04012.
11. Bamber JL, Siegert MJ, Griggs JA, Marshall SJ, Spada G (2013) Paleofluvial megacanyon beneath the central Greenland ice sheet. *Science* 341(6149):997–999.
12. Box JE, Ski K (2007) Remote sounding of Greenland supraglacial melt lakes: Implications for subglacial hydraulics. *J Glaciol* 53:257–265.
13. Selmes N, Murray T, James TD (2011) Fast draining lakes on the Greenland Ice Sheet. *Geophys Res Lett* 38:1–5.
14. Leeson AA, et al. (2013) A comparison of supraglacial lake observations derived from MODIS imagery at the western margin of the Greenland ice sheet. *J Glaciol* 59: 1179–1188.
15. Fitzpatrick AAW, et al. (2014) A decade (2002–2012) of supraglacial lake volume estimates across Russell Glacier, West Greenland. *Cryosph* 8:107–121.
16. Catania GA, Neumann TA, Price SF (2008) Characterizing englacial drainage in the ablation zone of the Greenland ice sheet. *J Glaciol* 54:567–578.
17. Das SB, et al. (2008) Fracture propagation to the base of the Greenland Ice Sheet during supraglacial lake drainage. *Science* 320(5877):778–781.
18. Schoof C (2010) Ice-sheet acceleration driven by melt supply variability. *Nature* 468(7325):803–806.
19. Palmer S, Shepherd A, Nienow P, Joughin I (2011) Seasonal speedup of the Greenland Ice Sheet linked to routing of surface water. *Earth Planet Sci Lett* 302:423–428.
20. Sundal AV, et al. (2011) Melt-induced speed-up of Greenland ice sheet offset by efficient subglacial drainage. *Nature* 469(7331):521–524.
21. Phillips T, Rajaram H, Colgan W, Steffen K, Abdalati W (2013) Evaluation of cryohydrologic warming as an explanation for increased ice velocities in the wet snow zone, Sermeq Avannarleq, West Greenland. *J Geophys Res Earth Surf* 118:1241–1256.
22. Yang K, Smith LC (2013) Supraglacial streams on the Greenland Ice Sheet delineated from combined spectral – shape information in high-resolution satellite imagery. *IEEE Geosci Remote Sens Lett* 10:801–805.
23. Rignot E, Velicogna I, van den Broeke MR, Monaghan A, Lenaerts JTM (2011) Acceleration of the contribution of the Greenland and Antarctic ice sheets to sea level rise. *Geophys Res Lett* 38:1–5.
24. Alley RB, Clark PU, Huybrechts P, Joughin I (2005) Ice-sheet and sea-level changes. *Science* 310:456–60.
25. Fettweis X, et al. (2013) Estimating the Greenland ice sheet surface mass balance contribution to future sea level rise using the regional atmospheric climate model MAR. *Cryosph* 7:469–489.
26. Vizcaíno M, Lipscomb WH, Sacks WJ, van den Broeke M (2014) Greenland Surface Mass Balance as Simulated by the Community Earth System Model. Part II: Twenty-First-Century Changes. *J Clim* 27:215–226.
27. Hall DK, et al. (2013) Variability in the surface temperature and melt extent of the Greenland ice sheet from MODIS. *Geophys Res Lett* 40:1–7.
28. Tedesco M, et al. (2013) Evidence and analysis of 2012 Greenland records from spaceborne observations, a regional climate model and reanalysis data. *Cryosph* 7: 615–630.
29. Legleiter CJ, Tedesco M, Smith LC, Behar E, Overstreet BT (2014) Mapping the bathymetry of supraglacial lakes and streams on the Greenland ice sheet using field measurements and high-resolution satellite images. *Cryosph* 8:215–228.
30. Rennermalm AK, et al. (2013) Evidence of meltwater retention within the Greenland ice sheet. *Cryosph* 7:1433–1445.
31. Andrews LC, et al. (2014) Direct observations of evolving subglacial drainage beneath the Greenland Ice Sheet. *Nature* 514(7520):80–83.
32. Zwally HJ, et al. (2002) Surface melt-induced acceleration of Greenland ice-sheet flow. *Science* 297(5579):218–222.
33. Sasgen I, et al. (2012) Timing and origin of recent regional ice-mass loss in Greenland. *Earth Planet Sci Lett* 333-334:293–303.